Computers & Industrial Engineering 173 (2022) 108679

Contents lists available at ScienceDirect

Computers & Industrial Engineering

journal homepage: www.elsevier.com/locate/caie

A novel multi-objective optimization model for the vehicle routing problem with drone delivery and dynamic flight endurance

Shuai Zhang, Siliang Liu, Weibo Xu, Wanru Wang *

School of Information Management and Artificial Intelligence, Zhejiang University of Finance and Economics, Hangzhou 310018, China

ARTICLE INFO

Keywords:
Multi-objective optimization
Vehicle routing problem with drone delivery
Dynamic flight endurance
Extended non-dominated sorting genetic algorithm

ABSTRACT

With growing environmental concerns and tough carbon–neutral objectives, logistics providers have to consider not only economic benefits but also environmental impact in the delivery process. This study proposes a novel multi-objective optimization model for the vehicle routing problem with drone delivery. The proposed model involves improving delivery efficiency and reducing environmental impact by extending the conventional ground vehicle (i.e. truck) delivery model with the implementation of drone delivery as well as the optimization of the total energy consumption of trucks. Drones need to collaborate with trucks to serve customers because of their limited flight endurance. Moreover, the fact that flight endurance is dynamic and influenced by the loading rate of drones is also considered to satisfy practical application scenarios. An extended non-dominated sorting genetic algorithm is presented to solve the proposed model. A new encoding and decoding method is incorporated to represent multiple feasible routes of drones and trucks, several crossover and mutation operators are integrated to accelerate the algorithmic convergence, and a multi-dimensional local search strategy is employed to enhance the diversity of population. Finally, the experimental results demonstrate that the presented algorithm is effective in obtaining high-quality non-dominated solutions by comparing it with three other baseline multi-objective algorithms.

1. Introduction

Growing concerns about environmental issues have prompted many developed countries, as well as some developing countries, to achieve carbon–neutral objectives to deal with the global climate change. However, the transportation sector inevitably has a negative impact on the environment owing to the carbon emissions stemming from fossil energy consumption. Statistics provided by the International Energy Agency indicate that the transportation sector was the worst carbon emitter after the electricity and heat production sectors in 2018, accounting for 24.64 % of global carbon emissions (Wei et al., 2021). Furthermore, carbon emissions are expected to increase if there is no behavior change in the transportation sector (Tian et al., 2018). As transportation is an important facet of logistics, logistics providers have to consider not only economic benefits but also environmental impact in the delivery process.

For reducing environmental impact, logistics providers attempt to design routing schemes which incorporate environmentally-friendly practices. This problem and its variants can be referred to as green vehicle routing problems (Erdoğan & Miller-Hooks, 2012; Asghari & Al-e-hashem, 2021). Some studies have focused on using electric vehicles instead of internal combustion engine vehicles to serve customers (Schneider et al., 2014). Although electric vehicles have nearly zero environmental impact, recharging stations must be deployed along the routes to prevent delivery failures due to the limited driving range. Insufficient recharging stations hinder the widespread adoption of electric vehicles worldwide. Other studies have focused on minimizing the total energy consumption or carbon emissions of vehicles during the delivery process (Kara et al., 2007; Wang et al., 2019). In general, the carbon emissions of vehicles are influenced by their energy consumption, which is primarily related to the travel distance and load. Thus, routing schemes with minimum total energy consumption or carbon emissions are not necessarily those with minimal economic costs.

For achieving economic benefits, logistics providers seek to leverage emerging technologies to improve their delivery efficiency and enhance their core competencies. For example, in recent years, drones have been widely used as a promising delivery tool for parcels. The delivery cost per unit of drones is relatively inexpensive because drones perform tasks

* Corresponding author.
E-mail addresses: zhangshuai@zufe.edu.cn (S. Zhang), liusiliang@zufe.edu.cn (S. Liu), weberxu5610@zufe.edu.cn (W. Xu), wanruwang@zufe.edu.cn (W. Wang).

https://doi.org/10.1016/j.cie.2022.108679
Received 11 February 2022; Received in revised form 18 September 2022; Accepted 20 September 2022
Available online 24 September 2022

autonomously, implying reduced labor costs for the delivery process (Agatz et al., 2018). In general, drones need to collaborate with ground vehicle (i.e. truck) to compensate for their shortcomings in flight endurance and load capacity, thereby leveraging their advantages of high delivery speed and low delivery costs. This hybrid delivery model of trucks and drones reduces not only delivery time (Moshref-Javadi et al., 2021) but also delivery costs (Ha et al., 2018), compared with the conventional truck-only delivery model.

Minimization of delivery completion time or delivery costs is a major optimization objective for hybrid delivery models of trucks and drones (Chung et al., 2020), and only few studies have considered minimization of the impact of hybrid delivery models on the environment. Chiang et al. (2019) proposed a green truck-drone delivery model to reduce the environmental impact by minimizing the total carbon emissions. However, this model only focuses on environmental efficiency with economic benefits sacrificed.

In addition, measuring the environmental impact of the overall delivery model by calculating the amount of carbon emissions is complex. As fossil energy consumption is roughly proportional to carbon emissions for a given vehicle (Turkensteen, 2017), indirectly measuring the environmental impact of the overall delivery model with total energy consumption has been widely recognized. Therefore, in this study, the total energy consumption of trucks is used to measure the environmental impact of the overall delivery model because drones are driven by electricity which produces nearly zero environmental impact. According to Jabir et al. (2015), energy consumption reduction and economic cost savings are two conflicting objectives in the delivery process. This motivated us to propose a novel multi-objective optimization model for the vehicle routing problem with drone delivery (MOVRPDD), where two economic objectives—total delivery costs and total delivery time—and one environmental objective—the total energy consumption of trucks— are considered. Furthermore, based on the fact that the less loaded drones have longer flight endurance than the fully loaded drones, the proposed model also considers the dynamic flight endurance of drones, which is influenced by their loading rate.

The main contributions of this study are as follows:

- A novel multi-objective optimization model for the vehicle routing problem with drone delivery is proposed with regard to economic benefits and environmental impact.
- The maximum flight endurance of the drones is dynamically adjusted by their loading rate to satisfy practical application scenarios.
- An extended non-dominated sorting genetic algorithm is proposed, which includes a new encoding and decoding method to represent multiple feasible routes of drones and trucks, several crossover and mutation operators to accelerate algorithmic convergence, and a multi-dimensional local search strategy to enhance the diversity of population.

The remainder of this paper is organized as follows. Section 2 discusses the relevant literature. In Section 3, the MOVRPDD model is established. Section 4 presents the basic non-dominated sorting genetic algorithm as well as its extension for solving MOVRPDD. In Section 5, the experimental results are discussed. Section 6 draws the conclusions.

2. Related work

This section introduces two types of work related to MOVRPDD: green vehicle routing problems, and vehicle routing problems with drone delivery.

2.1. Green vehicle routing problems

Green vehicle routing problems focus on optimizing the routes of vehicles that serve a set of customers with minimal environmental impact. Two different approaches are used to mitigate the environmental impacts of delivery operations.

One approach is to proactively abandon the use of conventional internal combustion engine vehicles (ICEVs), which are not conducive to the environment. For example, Erdoğan and Miller-Hooks (2012) used alternative-fuel vehicles instead of ICEVs to achieve delivery tasks and dealt with the difficulties in limited driving range and refueling infrastructure. Schneider et al. (2014) employed electric vehicles with limited capacity and driving range instead of ICEVs to serve customers within the time window; accordingly, they proposed an appropriate recharging scheme. In our previous work (Zhang et al., 2020), the authors solved the electric vehicle routing problem by handling uncertainty factors such as service time, battery energy consumption and travel time through a fuzzy optimization model. However, owing to limited refueling (or recharging) infrastructure, deploying alternative-fuel (or electric) vehicles on a large scale in practical logistics delivery is difficult.

Another approach is to incorporate components related to environmental impacts in the optimization objective. For example, Xiao et al. (2012) investigated the capacitated vehicle routing problem with minimum energy consumption by exploring the relationship between energy consumption rates and loading factors. Xu et al. (2019) investigated the same problem and considered the non-linear variation of travel speed in energy consumption function. Li et al. (2018) formulated a heterogeneous fixed fleet vehicle routing problem with minimum costs, in which, the carbon emissions and energy consumption were translated into variable costs. Fan et al. (2021) investigated the multi-depot green vehicle routing problem with minimum costs, where the energy consumption costs were also considered and the energy consumption was affected by the load and road gradient. However, the above studies failed to consider the trade-off between environmental impact and economic benefits, focusing only on optimizing the single objective towards environmental impact.

Jabir et al. (2015) proposed a multi-objective optimization model for the green vehicle routing problem; this model was aimed at resolving the conflict between carbon emission minimization and delivery cost minimization. Li et al. (2019) investigated a multi-depot green vehicle routing model that optimized multiple objectives of maximizing revenue and minimizing costs, time, and emissions simultaneously. However, the above studies only used the multi-objective optimization model to determine numerous alternative routing schemes that deal with the trade-offs between economic benefits and environmental impact, but failed to improve the delivery efficiency and reduce environmental impact simultaneously.

Thus, this study proposes a novel multi-objective optimization model that incorporates emerging delivery tools (drones) into the conventional green vehicle routing problem to better curb delivery costs increase while reducing environmental impact.

2.2. Vehicle routing problems with drone delivery

In recent years, drones have been considered a promising delivery tool owing to their high flight speed and low delivery cost and have drawn the attention of many researchers. Murray & Chu (2015) proposed a collaborative delivery problem involving trucks and drones, in which a large-capacity low-speed truck and a small-capacity high-speed drone work together to deliver parcels to customers, thereby minimizing delivery time. This problem is called the traveling salesman problem with drones (TSP-D). On this basis, Ha et al. (2018) studied a variant of the TSP-D that aimed to minimize the total costs, including delivery costs and penalty costs incurred by the waiting time of trucks. The above studies illustrated that the use of drones can effectively reduce total delivery costs or the total delivery time compared with conventional truck-only delivery models. However, delivery models with a single truck and drone are not productive for logistics providers.

Thus, some researchers have investigated relatively complex and productive delivery models. For example, Kitjacharoenchai et al. (2019)

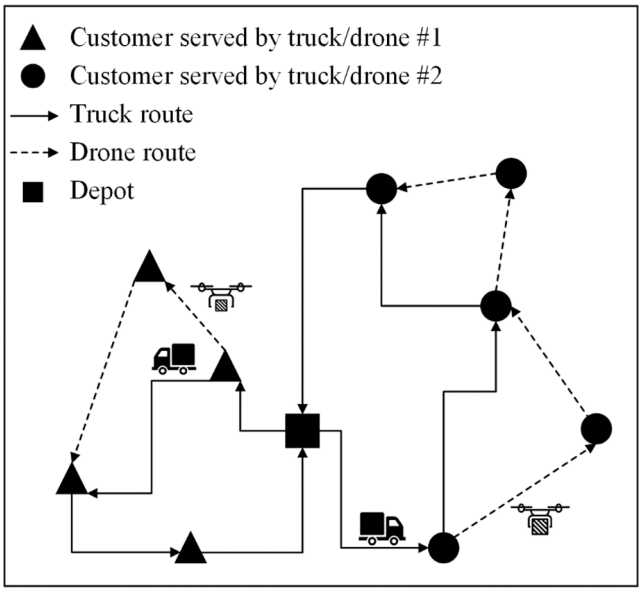

Fig. 1. Schematic of the MOVRPDD model.

studied the multiple traveling salesman problem with drones, which extended the TSP-D and allowed multiple trucks and drones for delivery. Murray & Raj (2020) proposed a collaborative delivery model involving a truck and a fleet of drones and analyzed the potential time savings associated with the use of multiple drones. Karak & Abdelghan (2019) proposed a vehicle-drone "mothership" system in which a truck was used to carry multiple drones and drones provided pick-up or delivery services to the customers. Wang et al. (2017) studied the vehicle routing problem with drones, in which a fleet of drone-equipped trucks delivered parcels to customers; they conducted a series of experiments to investigate the maximum savings that could be obtained by using drones in a worst-case scenario. Li et al. (2020) studied the two-echelon vehicle routing problem with time windows and mobile satellites. In this problem the first echelon encompasses the delivery routes of the trucks (represented as mobile satellites) from the distribution center to customers, and the second echelon is the delivery routes of drones from mobile satellites to the customers and back to the mobile satellites.

However, the above studies only explored single-objective optimization models for the vehicle routing problem with drone delivery based on economic benefits, such as minimum delivery costs or time. Although Das et al. (2021) developed a multi-objective optimization model integrating the objectives of minimizing travel costs and maximizing the level of customer service in terms of timely delivery, the environmental impact was not considered. Thus, this study proposes a multi-objective optimization model that considers both economic benefits and environmental impact, which minimizes the total delivery costs, total delivery time, and total energy consumption of trucks simultaneously.

In addition, the existing studies typically assumed that the maximum flight endurance of drones is constant; however, in reality, it is dynamic and influenced by the loading rate of drones. According to Dorling et al. (2017), the energy consumption of drones varies approximately linearly with payload weight. The heavier the loading weight of the drone, the faster the drone battery will be depleted. Therefore, to meet the requirements for practical application, the proposed model in this study considers dynamic flight endurance under different loading rates of drones.

3. Multi-objective vehicle routing problem with drone delivery and dynamic flight endurance

3.1. Problem statement

Fig. 1 illustrates the MOVRPDD model. A fleet of trucks leaves the depot to serve all customers sequentially. Each truck in the fleet is equipped with a drone, and either serves the customer directly or by launching and retrieving the drone. For multiple trucks and drones, appropriate routes should be determined to obtain an optimal delivery solution that minimizes the total delivery costs, total delivery time, and total energy consumption.

In the proposed MOVRPDD model, the following assumptions are given: (1) The maximum flight endurance of the drone is dynamic and depends on the loading rate of the drone. (2) The launching and retrieval times of drones are ignored. (3) The routes of trucks are measured using the Manhattan distance because of the restrictions of urban road networks. (4) A drone travels in a straight line between two nodes, and its route is measured using the Euclidean distance. (5) The routes of the drone consist only of horizontal travel; vertical travel is not considered. (6) The drone cannot be re-launched until it is retrieved.

3.2. Notations

To establish the MOVRPDD model, the sets, parameters, and variables are defined as follows:

(1) Sets	
N:	The set of nodes representing all customers, $N = \{1, 2, \ldots, n\}$.
N_0:	The set of nodes including all customers and depot node 0 where trucks leave from, $N_0 = \{0, 1, 2, \ldots, n\}$.
N_+:	The set of nodes including all customers and depot node $n+1$ where trucks return, $N_+ = \{1, 2, \ldots, n, n+1\}$. The positions of the depot node 0 and node $n+1$ are the same.
V:	The set of homogeneous trucks with drones, $V = \{1, 2, \ldots, v\}$.
(2) Parameters	
q_i:	Demand for customer node i.
d_{ij}^M:	Manhattan distance for the truck to travel from node i to node j. If the positions of nodes i and j are (a_1, b_1) and (a_2, b_2), respectively, then$d_{ij}^M = \lvert a_1 - a_2\rvert + \lvert b_1 - b_2\rvert$.
d_{ij}^E:	Euclidean distance for the drone to travel from nodes i to j. If the positions of nodes i and j are (a_1, b_1) and (a_2, b_2), respectively, then$d_{ij}^E = \sqrt{(a_1 - a_2)^2 + (b_1 - b_2)^2}$.
E:	Maximum endurance of empty drones
Q_T:	Load capacity of trucks.
Q_D:	Load capacity of drones.
W_T:	Tare (empty) weight of trucks.
W_D:	Tare (empty) weight of drones.
C_T:	Travel cost of trucks per unit distance.
C_D:	Travel cost of drones per unit distance.
C_B:	Basis cost of using a truck equipped with a drone.
S_T:	Average travel speed of trucks.
S_D:	Average travel speed of drones.
M:	A large positive number.
(3) Variables	
x_{ij}^v:	A binary number that equals 1 if truck v travels from node i to node j, otherwise 0;$x_{ij}^v \in \{0, 1\}$.
y_{ijk}^v:	A binary number that equals 1 if drone v (equipped on truck v) is launched at node i, serves customer at node j, and is retrieved at node k, otherwise 0;$y_{ijk}^v \in \{0, 1\}$.
t_i^v:	The arrival time of truck v at node i.
$t_i^{'v}$:	The arrival time of drone v at node i.
ξ_{ij}^v:	The loading rate of drone v when it travels from node i to node j.
θ_{ij}^v:	Dynamic scaling factor of the maximum flight endurance of drone v when it travels from node i to node j.
E_{ijk}^v:	The expected maximum flight endurance of the loaded drone v when it is launched at node i, serves customer at node j, and is retrieved at node k.
W_{ij}^v:	Gross weight of loaded truck v when it travels from node i to node j.
p_{ij}^v:	The payload of truck v when it travels from node i to node j.
u_i^v:	The order of visitation of node i in the route of truck v.

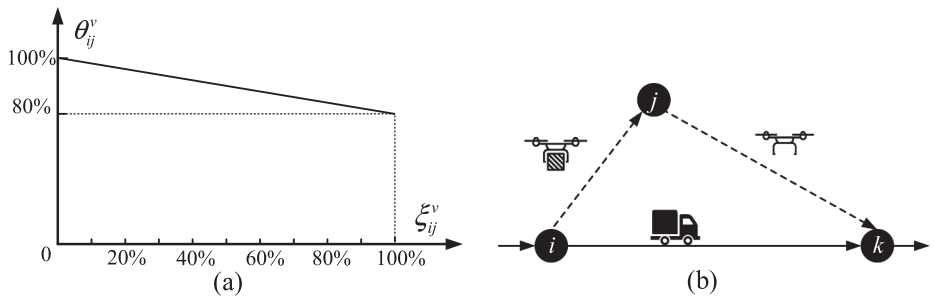

Fig. 2. Illustration of maximum flight endurance under different loading rates.

3.3. Mathematical model

(1) Calculation of intermediate variables

Before defining the optimization objective of the proposed model, some intermediate variables, which are influenced by the decision variables x_{ij}^v or y_{ijk}^v, are calculated first.

The loading rate ξ_{ij}^v is calculated using Eq. (1). Only when the drone v is launched from node i and serves customer j, i.e., $\sum_{k\in N_+} y_{ijk}^v = 1$, the value of ξ_{ij}^v equals the demand of customer j divided by the load capacity of the drones.

$$\xi_{ij}^v = \begin{cases} \frac{q_j}{Q_D} \sum_{k\in N_+} y_{ijk}^v = 1 \\ 0 \sum_{k\in N_+} y_{ijk}^v = 0 \end{cases} \tag{1}$$

Because the loading rates ξ_{ij}^v will negatively influence the maximum flight endurance of the drones, this study assumes that the maximum flight endurance of drones decreases linearly with an increase in their loading rate; when the drones are fully loaded, their maximum flight endurance is reduced to 80 % of the maximum flight endurance of empty drones. Therefore, the dynamic scaling factor θ_{ij}^v for the maximum flight endurance of the loaded drones is calculated using Eq. (2). Fig. 2(a) shows the decreasing trend of θ_{ij}^v with an increase in loading rate ξ_{ij}^v. For a certain flight with a drone starting from node i, serving a customer at node j, and ending at node k, i.e., $y_{ijk}^v = 1$, as shown in Fig. 2(b), the expected maximum flight endurance E_{ijk}^v of this drone is calculated using Eq. (3). This flight consists of two phases: the drone first travels from node i to node j with a certain loading rate and then travels from node j to node k with an empty load. Thus, the value of E_{ijk}^v equals the weighted sum of the maximum flight endurance in these two phases.

$$\theta_{ij}^v = 100\% - 0.2\xi_{ij}^v \tag{2}$$

$$E_{ijk}^v = \begin{cases} \left(\left(\frac{d_{ij}^E}{d_{ij}^E + d_{jk}^E}\right)\theta_{ij}^v + \left(\frac{d_{jk}^E}{d_{ij}^E + d_{jk}^E}\right)\right) E\ y_{ijk}^v = 1 \\ 0\ y_{ijk}^v = 0 \end{cases} \tag{3}$$

The expression of the gross weight of a truck during delivery was inspired by Chiang et al. (2019), and this study extends the original expression to accommodate delivery models with multiple trucks and drones, as described in Eq. (4). Only if the truck v travels from node i to node j, i.e., x_{ij}^v=1, the value of W_{ij}^v includes the tare weight of the truck W_T, the weight of the payload p_{ij}^v, and the tare weight of the drone W_D, if applicable. In particular, if the drone is not on the truck, i.e., $\sum_{m\in N} y_{imj}^v$=1, the value of W_{ij}^v equals the sum of the first and second items.

$$W_{ij}^v = \begin{cases} W_T + p_{ij}^v + W_D\left(1 - \sum_{m\in N} y_{imj}^v\right)\ x_{ij}^v = 1 \\ 0\ x_{ij}^v = 0 \end{cases} \tag{4}$$

(2) Objectives

The MOVRPDD model has three optimization objectives as shown below.

$$Min\ f_1 = \sum_{v\in V}\sum_{i\in N_0}\sum_{j\in N_+} d_{ij}^M W_{ij}^v x_{ij}^v \tag{5}$$

$$Min\ f_2 = \sum_{v\in V}\left(\sum_{i\in N_0}\sum_{j\in N_+} C_T d_{ij}^M x_{ij}^v + \sum_{i\in N_0}\sum_{j\in N}\sum_{k\in N_+} C_D(d_{ij}^E + d_{jk}^E) y_{ijk}^v\right) + \sum_{v\in V}\sum_{j\in N_+} x_{0j}^v C_B \tag{6}$$

$$Min\ f_3 = \max_{v\in V}\{t_{n+1}^v\} \tag{7}$$

The environmental objective f_1 is used to minimize the total energy consumption. Here only the energy consumption of trucks is considered because drones are powered by electricity, which has nearly zero impact on the environment. The energy consumption of trucks is related to their load and distance traveled (Kara et al., 2007) and the calculation is given by Eq. (5). Economic objectives f_2 and f_3 are used to minimize the total delivery cost and total delivery time, respectively. The calculation of the total delivery cost in Eq. (6) includes both changeable costs related to the delivery routes of trucks and drones and the basis costs related to the number of trucks with drones used. The total delivery time in Eq. (7) indicates the arrival time of the latest truck that arrives at the depot after all customers are served.

(3) Constraints

The MOVRPDD model must satisfy the following constraints:

$$\sum_{v\in V}\sum_{i\in N_0} x_{ij}^v + \sum_{v\in V}\sum_{i\in N_0}\sum_{k\in N_+} y_{ijk}^v = 1; \forall j \in N \tag{8}$$

$$\sum_{j\in N_+} x_{0j}^v \le 1; \forall v \in V \tag{9}$$

$$\sum_{i\in N_0} x_{i(n+1)}^v \le 1; \forall v \in V \tag{10}$$

$$x_{0(n+1)}^v = 0; \forall v \in V \tag{11}$$

$$\sum_{\substack{j\in N \\ j\neq i}}\sum_{\substack{k\in N_+ \\ k\neq j}} y_{ijk}^v \le 1; \forall v \in V, i \in N_0 \tag{12}$$

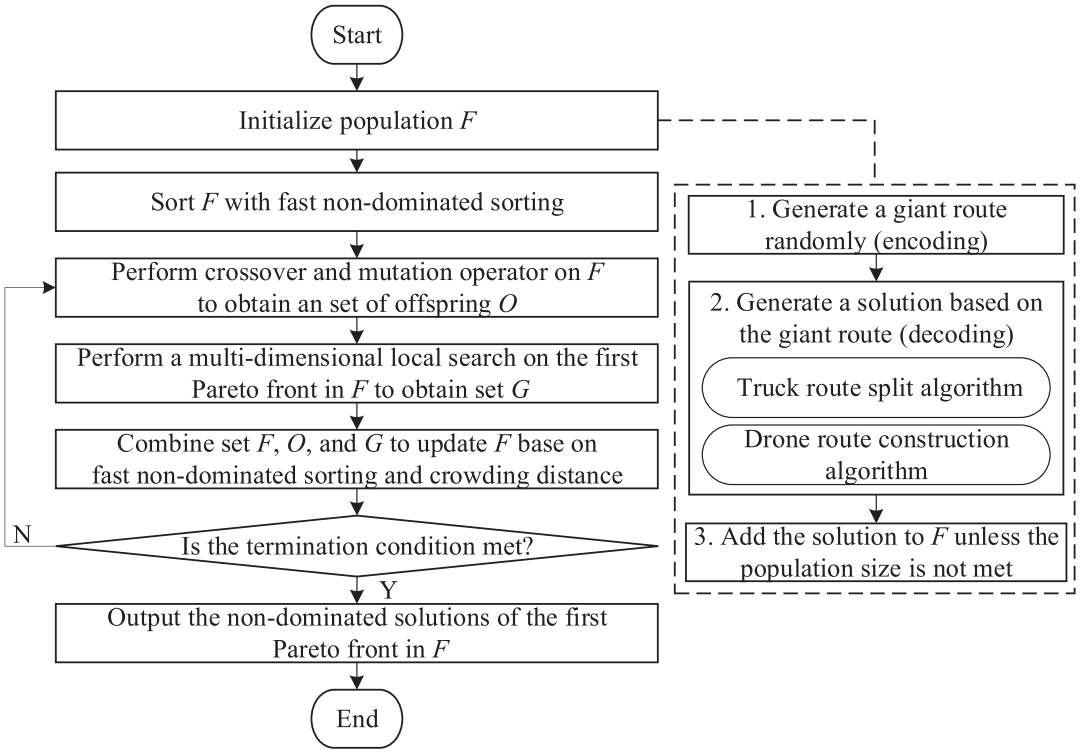

Fig. 3. Framework of the ENSGA-II algorithm.

$$\sum_{\substack{i\in N_0\\ i\neq j}}\sum_{\substack{j\in N\\ j\neq k}} y_{ijk}^{v} \le 1; \forall v \in V, k \in N_+ \tag{13}$$

$$\sum_{\substack{i\in N_0\\ i\neq j}}\sum_{\substack{k\in N_+\\ k\neq i}} y_{ijk}^{v} q_j \le Q_D; \forall j \in N, v \in V \tag{14}$$

$$\sum_{j\in N}\left(\sum_{i\in N_0} x_{ij}^{v} q_j + \sum_{i\in N_0}\sum_{k\in N_+} y_{ijk}^{v} q_j\right) \le Q_T; \forall v \in V \tag{15}$$

$$2y_{ijk}^{v} \le \sum_{\substack{h\in N_0\\ h\neq i}} x_{hi}^{v} + \sum_{\substack{l\in N\\ l\neq k}} x_{lk}^{v}; \forall i \in N, j \in \{N : j \neq i\}, k \in \{N_+ : k \neq j\}, v \in V \tag{16}$$

$$u_k^{v} - u_i^{v} \ge 1 - M\left(1 - \sum_{j\in N} y_{ijk}^{v}\right); \forall i \in N,\ k \in \{N_+ : k \neq i\},\ v \in V \tag{17}$$

$$t_i'^{\,v} \ge t_i^{v} - M\Big(1 - \sum_{\substack{j\in N\\ j\neq i}}\sum_{\substack{k\in N_+\\ k\neq j}} y_{ijk}^{v}\Big); \forall i \in N, v \in V \tag{18}$$

$$t_i'^{\,v} \le t_i^{v} + M\Big(1 - \sum_{\substack{j\in N\\ j\neq i}}\sum_{\substack{k\in N_+\\ k\neq j}} y_{ijk}^{v}\Big); \forall i \in N, v \in V \tag{19}$$

$$t_k'^{\,v} \ge t_k^{v} - M\Big(1 - \sum_{\substack{i\in N_0\\ i\neq j}}\sum_{\substack{j\in N\\ j\neq k}} y_{ijk}^{v}\Big); \forall k \in N_+, v \in V \tag{20}$$

$$t_k'^{\,v} \le t_k^{v} + M\Big(1 - \sum_{\substack{i\in N_0\\ i\neq j}}\sum_{\substack{j\in N\\ j\neq k}} y_{ijk}^{v}\Big); \forall k \in N_+, v \in V \tag{21}$$

$$t_j^{v} \ge t_i^{v} + \frac{d_{ij}^{M}}{S_T} - M\left(1 - x_{ij}^{v}\right);\ \forall i \in N,\ j \in \{N : j \neq i\},\ v \in V \tag{22}$$

$$t_j'^{\,v} \ge t_i'^{\,v} + \frac{d_{ij}^{E}}{S_D} - M\Big(1 - \sum_{k\in N_+} y_{ijk}^{v}\Big); \forall i \in N, j \in \{N : j \neq i\}, v \in V \tag{23}$$

$$t_k'^{\,v} \ge t_j'^{\,v} + \frac{d_{jk}^{E}}{S_D} - M\Big(1 - \sum_{i\in N_0} y_{ijk}^{v}\Big); \forall j \in N, k \in \{N_+ : k \neq j\}, v \in V \tag{24}$$

$$t_k'^{\,v} - t_i'^{\,v} \le \sum_{j\in N} E_{ijk}^{v} + M\Big(1 - \sum_{j\in N} y_{ijk}^{v}\Big); \forall k \in N_+, i \in \{N : i \neq k\}, v \in V \tag{25}$$

Constraint (8) ensures that all customers are served by trucks or drones. Constraints (9)–(10) ensure that each truck leaves from and returns to the depot at most once. Trucks are prohibited from traveling directly from depot to depot as described in Eq. (11). Constraints (12)–(13) ensure that each drone is launched or retrieved at most once at all customers and depot nodes. Constraint (14) ensures that each drone is not loaded beyond its load capacity during flight. Constraint (15) ensures that each truck does not exceed its load capacity during delivery. Constraint (16) ensures that if the drone is launched at node i and retrieved at node k, the truck must pass through both nodes. Constraint (17) ensures that the delivery sequence of the trucks is consistent with that of the drones. Constraints (18)–(21) ensure that the arrival times of each truck and its corresponding drone at the launch and retrieval nodes are synchronized. Constraints (22)–(24) ensure that the arrival times of the trucks and drones are reasonable during movement. Constraint (25) ensures that the flight time of the drone does not exceed its maximum endurance.

4. Proposed method

In this section, first, the classic non-dominated sorting genetic algorithm (NSGA-II) is described. Then, the extended non-dominated sorting genetic algorithm (ENSGA-II) is proposed for solving the

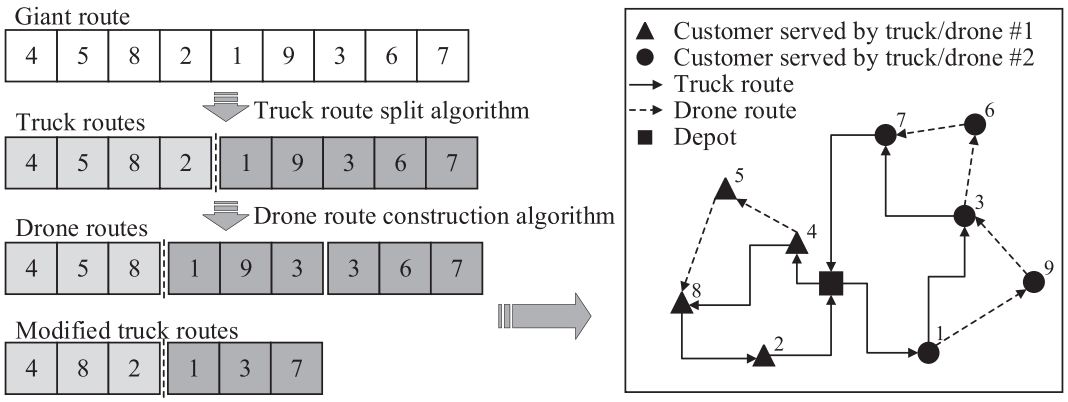

Fig. 4. Illustration of the encoding and decoding of the MOVRPDD solution.

MOVRPDD model.

4.1. Introduction of NSGA-II algorithm

The NSGA-II proposed by Deb et al. (2002) is commonly used to solve multi-objective optimization problems. As no solution can provide the best performance for all objectives in multi-objective optimization problems, NSGA-II aims to find the Pareto-optimal solutions whose one objective cannot be improved without sacrificing at least one of the other objectives. Thus, the population update mechanism of NSGA-II is quite different from that of the popular genetic algorithm proposed by Goldberg (1989). To update the population, NSGA-II sorts the new solutions generated by crossover and mutation based on Pareto dominance and then selects them based on the crowding distance. Fast non-dominated sorting and crowding distance calculation are two important components of the algorithm.

In fast non-dominated sorting, the population is iteratively sorted into different Pareto fronts. Solutions not dominated by other solutions in the population constitute the first Pareto front. Similarly, the second Pareto front is found in the remaining solutions of the population. The same process is repeated until all solutions are divided into different Pareto fronts.

The process of crowding distance calculation (Deb et al. 2002) is described as follows. First, solutions in the same Pareto front are sorted in ascending order of the objective value according to each optimization objective. Second, for each optimization objective, the distance value of the first and last solutions is set to infinity, and the distance value of other solutions is equal to the absolute value of the objective difference between two adjacent solutions. Finally, the total crowding distance of each solution is the sum of its corresponding distance values under each optimization objective.

When updating the population, the Pareto fronts in the population are selected from low to high, and a solution with a higher crowding distance in the same Pareto front is preferable.

4.2. ENSGA-II algorithm for solving the MOVRPDD model

To adapt the NSGA-II algorithm to the MOVRPDD model, this study proposes an ENSGA-II algorithm that has three extensions to the classic NSGA-II algorithm: 1) a new encoding and decoding method is presented to ensure the generation of feasible and high-quality solutions during evolution, 2) multiple crossover and mutation operators are integrated to accelerate the algorithmic convergence, and 3) a multi-dimensional local search strategy is designed to increase the diversity of non-dominated solutions in the population. The framework of the ENSGA-II algorithm is shown in Fig. 3.

4.2.1. Encoding and decoding

The MOVRPDD solution is complicated because it consists of two types of routes for trucks and drones. In this study, giant route encoding was employed to represent the MOVRPDD solution in a compact way. The giant route is a sequence containing all customer nodes, which makes the crossover operation easy to be implemented (Zhang et al., 2019). However, the route only represents multiple truck routes in previous works (Prins, 2004; Zhang et al., 2019) and cannot be directly evaluated before decoding. Thus, a new encoding and decoding method is proposed to enable the giant route to represent both truck and drone routes of the MOVRPDD solution. As shown in Fig. 4, the giant route must first be transformed into truck routes by employing the truck route split algorithm (Prins, 2004). Then, based on truck routes, drone routes and modified truck routes are obtained by proposing a new drone route construction algorithm. Notably, the execution results of the truck route split algorithm and drone route construction algorithm are deterministic, and a certain giant route can uniquely represent a certain MOVRPDD solution with one-to-one mapping.

For example, referring to Fig. 4, the giant route [4, 5, 8, 2, 1, 9, 3, 6, 7] is first transformed into the routes of truck #1 [4, 5, 8, 2] and truck #2 [1, 9, 3, 6, 7]. Searching for flights on the route of truck #1, the route of drone #1 [4, 5, 8] is obtained, including the launch node, customer node, and retrieval node. Searching for flights on the route of truck #2, the route of drone #2 [[1, 9, 3], [3, 6, 7]], which consists of two flight routes [1, 9, 3] and [3, 6, 7], is also obtained. Because customers #5, #9, and #6 are assigned to drone service, the routes of trucks #1 and #2 are finally modified to [4, 8, 2] and [1, 3, 7], respectively.

(1) Truck route split algorithm

The truck route split algorithm aims to split a given giant route into multiple feasible truck routes with the minimum total distance, which is essentially the tour splitting algorithm proposed by Prins (2004) to solve the capacitated vehicle routing problem. It was employed in this study to minimize the total delivery cost and delivery time (f_2 and f_3) of the MOVRPDD solution. The process of splitting multiple truck routes from a giant route, and the efficient implementation of the algorithm can be found in Prins et al. (2009).

(2) Drone route construction algorithm

The drone route construction algorithm is proposed in this study to construct the feasible drone routes with the most flights. This helps minimize the total energy consumption of trucks (f_1) of the MOVRPDD solution. As the total energy consumption of trucks is related to their load and distance traveled, when as many customers as possible on the original truck routes are assigned to drone service, the load and distance traveled of the truck will be reduced, and correspondingly, the total

truck energy consumption will be reduced.

In essence, because the flight is the basic unit that constitutes the drone route, constructing the drone route entails sequentially searching for flights on truck route. The search procedure of flights on the truck route is described as follows (referring to Fig. 5).

Each flight has the structure [*la*, *cust*, *re*], where *la* denotes the launch node, *cust* denotes the customer node, and *re* denotes the retrieval node. *T* denotes the search range of flight on the truck route. Initially, the search range is the entire truck route.

Step 1: From left to right, select the customer on the truck route whose demand does not exceed the maximum load capacity of the drone as *cust* node. Ensure that the selected *cust* node is in search range *T* and is not the beginning node. Then the feasible flight that serves the given *cust* node will be searched for by Step 2 and Step 3.

Step 2: *la_list* is the multiple potential launch nodes for a drone. Select the node in *la_list* that has the minimum Euclidean distance to the customer node *cust* as the launch node *la*. This helps to minimize the distance of flight.

Step 3: *re_list* is the multiple potential retrieval nodes for a drone. Select the node in *re_list* that is the most closed to the customer node *cust* as the retrieval node *re*. If the flight [*la, cust, re*] does not exceed the dynamic endurance of the drone, the current search is completed. This corresponding flight will be added to the drone route and then the search range *T* will be narrowed to the segment which contains the *re* node and the nodes after it for the next flight search.

Note that the reason for selecting the node that is the most closed to the *cust* node in *re_list* as *re* node is to narrow the search range *T* for the next flight slowly and provide a relatively larger search range for the next flight, thereby facilitating the construction of the drone route with the most flights.

The pseudocode of the drone route construction algorithm is shown in Algorithm 1, comprising two phases: constructing the drone route based on the truck route (lines 1–22) and modifying the truck route based on the drone route (lines 23–26).

Algorithm 1: Drone route construction algorithm

Input: Truck route, T_{route};
Output: Drone route, D_{route}; Modified truck route, $\widetilde{T}_{route}$;

```
1  D_route ← ∅;
2  la, cust, re ← 0;
3  flight ← [la, cust, re];
4  T ← T_route;
5  for each customer c in T_route do
6      if the demand of c doesn't exceed the maximum load capacity of the drone then
7          if c in T and c is not the beginning node of T then
8              cust ← c;
9              la_list ← the segment of T which contains nodes before c;
10             la ← the node that has the minimum Euclidean distance from c in la_list;
11             re_list ← the segment of T which contains nodes after c;
12             for each node in re_list do
13                 re ← node;
14                 if flight doesn't exceed the dynamic endurance of drone then
15                     D_route ← D_route ∪ flight;
16                     T ← the segment of T which contains re and the node after re;
17                     break;
18                 end
19             end
20         end
21     end
22 end
23 T̃_route ← T_route;
24 for each flight in D_route do
25     remove cust in flight from T̃_route;
26 end
27 return D_route, T̃_route;
```

4.2.2. Crossover and mutation operation

To accelerate the algorithmic convergence, the partially matching crossover (PMX) operator and the order crossover (OX) operator (Potvin, 1996) are randomly used in the crossover operation of ENSGA-II. Examples of crossover operations are shown in Fig. 6. Several adjacent customers on old giant routes are randomly chosen first, which are called crossover segments (distinguished by color). The PMX operator is to replace the crossover segments on old giant route #1 with those on old giant route #2 to create a new giant route. Additionally, a matching relationship between the crossover segments is used to eliminate duplicated customers on the new giant route. For example, customer #8 is matched with customer #7 (denoted as $8 \leftrightarrow 7$). $8 \leftrightarrow 7$ indicates that if there is a duplicate customer #7 on the new giant route, it will be replaced by customer #8 to eliminate the duplication, and vice versa. Similarly, $5 \leftrightarrow 2$, $2 \leftrightarrow 1$ and $1 \leftrightarrow 9$ indicate duplicate customer #5 on the new giant route can be replaced by customer #2, customer #1, or customer #9. Since customer #2 and customer #1 already exist on the new giant route, duplicate customer #5 will be replaced by customer #9. The OX operator is to preserve the crossover segments on the old giant route #1 to create a new giant route. Then, the remaining parts of the new giant route are filled orderly by customers on the old giant route #2 except for the duplicated customers on the new giant route.

In addition, swap, insert, and reverse mutation operators are randomly used in the mutation operation of ENSGA-II. Examples of mutation operations are shown in Fig. 7. The swap mutation operator swaps two customers on a giant route. The insert mutation operator inserts one customer in front of another customer on a giant route. The reverse mutation operator is used to reverse several adjacent customers on a giant route.

4.2.3. A multi-dimensional local search strategy

In order to increase the diversity of the population, a multi-dimensional local search strategy is designed in ENSGA-II to explore non-dominated solutions with better specific objective values. It is applied to the first Pareto front in the population, so-called F_1. The exploration of non-dominated solutions in F_1 is randomly performed by the swap, insert or reverse mutation operators. For each specific optimization objective, the resulting solutions with the better objective values will be selected to form the new set of non-dominated solutions G. The pseudocode of the multi-dimensional local search strategy is shown in Algorithm 2.

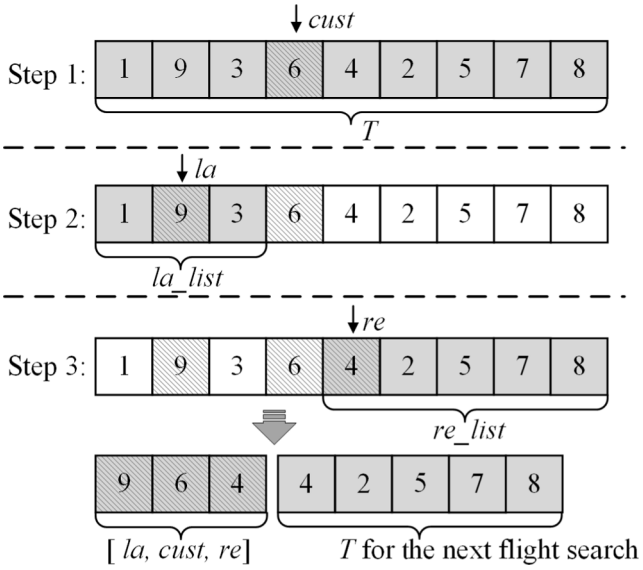

Fig. 5. Search procedure of flights on the truck route.

5. Numerical experiment

To evaluate the performance of the ENSGA-II algorithm for solving the MOVRPDD model, it was compared with some baseline multi-objective optimization algorithms. Owing to the complexity of the formulated MOVRPDD, no existing exact methods can be employed to solve it directly. Therefore, the classical and popular multi-objective optimization algorithms including NSGA-II, SPEA2 (Zitzler et al., 2002), and MOEA/D (Zhang & Li, 2007), were extended with the proposed encoding and decoding methods as well as multiple crossover and mutation operators first, and then compared with the proposed ENSGA-II algorithm. All algorithms were implemented in Python and experiments were conducted on a personal computer with a Windows 10 system, 3.60 GHz AMD Ryzen 5 3600 CPU and 32 GB of RAM.

5.1. Benchmark instance

Before evaluating the proposed ENSGA-II algorithm, new benchmark instances were generated to simulate real-world delivery scenarios. In

Algorithm 2: A multi-dimensional local search strategy

Input: the first Pareto front in population, F_1;
Output: a set of solutions, G;

```
G ← ∅;
for non-dominated solution s in F1 do
    for specific optimization objectives 1 to 3 do
        randomly perform a mutation operator on s to obtain s′;
        if specific objective value of s′ is better than that of s then
            G ← G ∪ s′;
        end
    end
end
return G;
```

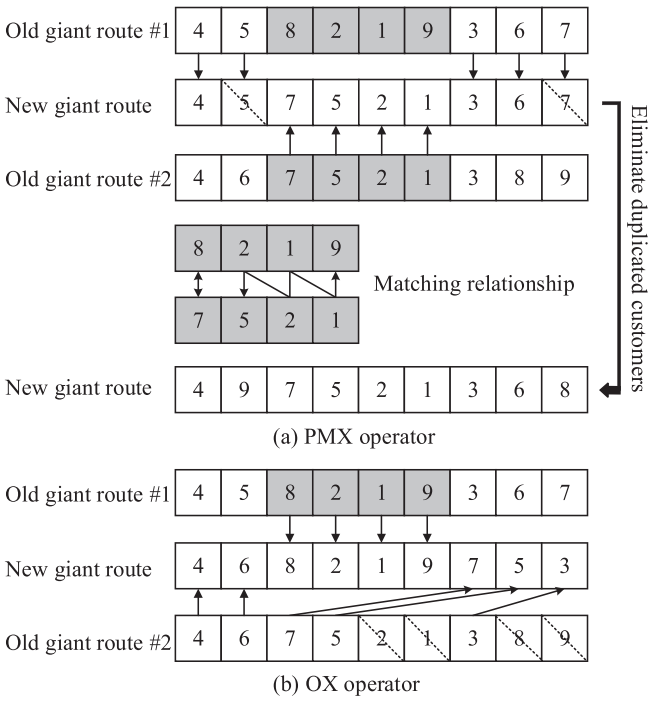

Fig. 6. Example of crossover operation.

these instances, the number of customers was set to 40, 80, 120, and 160, respectively. All customers and the depot were located in a square area. The vertical distance from the edge of the area to the center of the area was set to 20 km, 30 km, and 40 km, which represent the three different sizes of square areas respectively.

Because the maximum load capacity of drones cannot satisfy the demand of all customers in the real world, the percentage of customers that can be served by drones is assumed to be 30 %, 50 %, and 70 % respectively in these instances.

Because these instances involve different types of combinations (the number of customers, vertical distance from the edges of the square area to its center, and percentage of customers who can be served by drones), they can be intuitively named. For example, the instance "40-20-30 %" implies that there are 40 customers located in a square area, the vertical distance from the edge of the area to its center is 20 km, and only 30 % of the customers can be served by the drone.

Inspired by Sacramento et al. (2019), in these instances, assuming the maximum load capacity of drones is 5 kg, the demand of customers who can be served by drones obeys a uniform distribution of 0 to 5 kg, and the demand of customers who cannot be served by drones obeys a uniform distribution of 5 to 100 kg. More details of the instances are available in the figshare database (https://doi.org/10.6084/m9.figshare.17697209). The parameters involved in the MOVRPDD model are listed in Table 1.

Table 1
Parameter settings of the MOVRPDD model.

Parameter	Notation	Numerical value	Reference
Tare weight of trucks	W_T	1500 kg	
Maximum load capacity of trucks	Q_T	1000 kg	Li et al. (2020)
Tare weight of drones	W_D	25 kg	Trop (2016)
Maximum load capacity of drones	Q_D	5 kg	Trop (2016)
Travel cost of trucks per unit distance	C_T	25 monetary unit/km	Ha et al. (2018)
Travel cost of drones per unit distance	C_D	1 monetary unit/km	Ha et al. (2018)
Basis cost of using a truck equipped with a drone	C_B	500 monetary unit	Chiang et al. (2019)
Maximum endurance of empty drones	E	0.5 h	Trop (2016)
Average travel speed of trucks	S_T	60 km/h	Li et al. (2020)
Average travel speed of drones	S_D	65 km/h	Li et al. (2020)

Table 2
Algorithm-related parameter settings.

Algorithm	ENSGA-II	NSGA-II	SPEA2	MOEA\D
Iteration	500	500	500	500
Population size	80	80	80	80
Crossover rate	0.8	0.8	0.8	0.8
Mutation rate	0.2	0.2	0.2	0.2
Archive size	–	–	80	–
Neighborhood size of weight vector	–	–	–	5

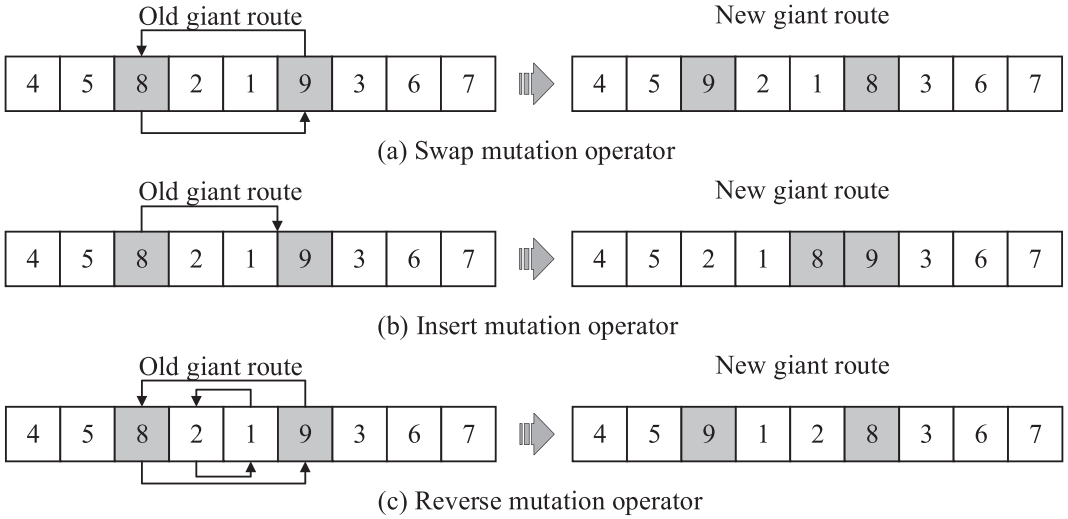

Fig. 7. Examples of mutation operation.

Table 3
Average results of IGD, HV, and Time of four algorithms on instances where the percentage of customers served by drones is 30%.

Instance	IGD				HV				Time(s)			
	E	N	S	M	E	N	S	M	E	N	S	M
40–20-30 %	**0.1180**	0.1691	0.1316	0.1390	**0.8880**	0.7650	0.8466	0.8286	1101.4	**442.6**	477.3	462.6
40–30-30 %	**0.1764**	0.2261	0.1930	0.2064	**0.8812**	0.7722	0.8507	0.8290	1088.9	**460.5**	501.8	480.8
40–40-30 %	**0.1527**	0.1847	0.2257	0.1823	**0.9585**	0.8249	0.7540	0.8445	1079.5	461.4	**453.4**	486.0
80–20-30 %	**0.1432**	0.2182	0.2125	0.2048	**0.9452**	0.7189	0.7353	0.7504	2178.1	**797.8**	912.6	1071.5
80–30-30 %	**0.1323**	0.1899	0.2275	0.1818	**0.9751**	0.7916	0.7302	0.8046	2318.4	**828.1**	907.1	1056.8
80–40-30 %	**0.2002**	0.3013	0.3363	0.2993	**0.9743**	0.8119	0.7539	0.8191	2240.3	**842.9**	1007.9	1035.8
120–20-30 %	**0.1631**	0.2072	0.3048	0.1871	**0.9590**	0.8188	0.7090	0.8516	3279.1	**1157.2**	1377.5	1612.4
120–30-30 %	**0.1646**	0.2397	0.2735	0.2199	**0.9740**	0.8227	0.7635	0.8408	3510.9	**1194.4**	1448.0	1648.9
120–40-30 %	**0.1284**	0.1952	0.2448	0.1720	**1.0178**	0.8085	0.7021	0.8231	3301.4	**1242.7**	1466.1	1613.6
160–20-30 %	**0.1181**	0.1742	0.2636	0.1653	**1.0008**	0.8913	0.6906	0.8945	4722.7	**1650.6**	2102.8	2233.5
160–30-30 %	**0.1823**	0.2956	0.3848	0.2555	**1.0319**	0.8650	0.6819	0.8846	4617.8	**1544.2**	2039.3	2245.0
160–40-30 %	**0.2332**	0.3495	0.4722	0.3295	**1.0297**	0.8203	0.6534	0.8479	4591.2	**1723.5**	2066.4	2308.0

Table 4
Average results of C-metric of ENSGA-II vs other algorithms on instances where the percentage of customers served by drones is 30%.

Instance	ENSGA-II (E) vs NSGA-II (N)		ENSGA-II (E) vs SPEA2 (S)		ENSGA-II (E) vs MOEA\D (M)	
	C (E, N)	C (N, E)	C (E, S)	C (S, E)	C (E, M)	C (M, E)
40–20-30 %	**0.3800**	0.1487	**0.4489**	0.1525	**0.4144**	0.1438
40–30-30 %	**0.1987**	0.0550	**0.3777**	0.1806	**0.4752**	0.1175
40–40-30 %	**0.5690**	0.1189	**0.6496**	0.0947	**0.5033**	0.0840
80–20-30 %	**0.5978**	0.0600	**0.6305**	0.0400	**0.5464**	0.1020
80–30-30 %	**0.5450**	0.0531	**0.6850**	0.0629	**0.5095**	0.0877
80–40-30 %	**0.4551**	0.1189	**0.6523**	0.0779	**0.4007**	0.1129
120–20-30 %	**0.3937**	0.1821	**0.7459**	0.0650	**0.3054**	0.2762
120–30-30 %	**0.4176**	0.2333	**0.6452**	0.1730	**0.3198**	0.2353
120–40-30 %	**0.5111**	0.1700	**0.7751**	0.0795	**0.3367**	0.1943
160–20-30 %	**0.3799**	0.2618	**0.7905**	0.0593	**0.3714**	0.2653
160–30-30 %	**0.5227**	0.2188	**0.8094**	0.0906	**0.3488**	0.2233
160–40-30 %	**0.6384**	0.1422	**0.8009**	0.0435	**0.5853**	0.1331

5.2. Performance indicator

The performance of a multi-objective algorithm needs to be comprehensively evaluated in terms of diversity and convergence. Three performance indicators were employed in this study, as follows:

(1) Inverted generational distance (IGD) proposed by Zhang and Li (2007) is an indicator that measures the diversity and convergence of the algorithm. IGD is the average minimum distance from each solution on the true Pareto front to non-dominated solutions obtained by the algorithm. A lower IGD value indicates a better performance of the algorithm.

(2) Hypervolume (HV) proposed by Zitzler and Thiele (1999) is another indicator that measures both the diversity and convergence of the algorithm. Assign a reference point, by which each non-dominated solution obtained by the algorithm can form a hypercube. HV is the area of the union of all the hypercubes. A larger HV value indicates a better performance of the algorithm.

(3) Coverage metric (C-metric) proposed by Zitzler and Thiele (1999) is an indicator for comparing the quality of two sets of non-dominated

Table 6
Average results of C-metric of ENSGA-II vs other algorithms on instances where the percentage of customers served by drones is 50%.

Instance	ENSGA-II (E) vs NSGA-II (N)		ENSGA-II (E) vs SPEA2 (S)		ENSGA-II (E) vs MOEA\D (M)	
	C (E, N)	C (N, E)	C (E, S)	C (S, E)	C (E, M)	C (M, E)
40–20-50 %	**0.3550**	0.1019	**0.4629**	0.1263	**0.5657**	0.1638
40–30-50 %	**0.2388**	0.1194	**0.3393**	0.1450	**0.5092**	0.1412
40–40-50 %	**0.4012**	0.1925	**0.5769**	0.0588	**0.4080**	0.2394
80–20-50 %	**0.5810**	0.0469	**0.6621**	0.0719	**0.4832**	0.0756
80–30-50 %	**0.6844**	0.0669	**0.6607**	0.1458	**0.7054**	0.1002
80–40-50 %	**0.5002**	0.0939	**0.6009**	0.0976	**0.5288**	0.1188
120–20-50 %	**0.5336**	0.1153	**0.8143**	0.0194	**0.4647**	0.1234
120–30-50 %	**0.6196**	0.1062	**0.7324**	0.0831	**0.5171**	0.1837
120–40-50 %	**0.4247**	0.2735	**0.6771**	0.1535	**0.5398**	0.2413
160–20-50 %	**0.5464**	0.1017	**0.7380**	0.0700	**0.5040**	0.1497
160–30-50 %	**0.5972**	0.1229	**0.7979**	0.0272	**0.4741**	0.1239
160–40-50 %	**0.6191**	0.1795	**0.7022**	0.0969	**0.4979**	0.1773

Table 5
Average results of IGD, HV, and Time of four algorithms on instances where the percentage of customers served by drones is 50%.

Instance	IGD				HV				Time(s)			
	E	N	S	M	E	N	S	M	E	N	S	M
40–20-50 %	**0.1923**	0.2444	0.2001	0.2323	**0.8892**	0.7286	0.8678	0.7883	1232.7	**480.3**	551.6	524.1
40–30-50 %	**0.1703**	0.2104	0.1777	0.1967	**0.8873**	0.7958	0.8742	0.8180	1178.7	505.7	559.6	**495.5**
40–40-50 %	**0.1775**	0.2051	0.2110	0.2114	**0.9108**	0.8142	0.7975	0.8194	1256.6	507.6	**486.7**	542.4
80–20-50 %	**0.1512**	0.2384	0.2756	0.1970	**1.0187**	0.7481	0.7284	0.8235	2556.2	**932.7**	1022.5	1224.2
80–30-50 %	**0.1855**	0.3161	0.2581	0.2951	**1.0224**	0.7037	0.8060	0.7058	2408.1	**1018.1**	1079.6	1251.6
80–40-50 %	**0.1608**	0.2416	0.2718	0.2426	**0.9656**	0.7438	0.7051	0.7442	2594.1	**979.0**	1046.2	1243.8
120–20-50 %	**0.2046**	0.2869	0.3642	0.2684	**1.0335**	0.8111	0.6933	0.8145	3872.2	**1380.7**	1606.3	1870.4
120–30-50 %	**0.1393**	0.2278	0.3283	0.2091	**1.0586**	0.8060	0.7007	0.8000	4002.4	**1400.3**	1673.5	1977.4
120–40-50 %	**0.2596**	0.3611	0.4092	0.3928	**0.9902**	0.8057	0.7140	0.7104	4499.9	**1616.8**	1866.2	2229.8
160–20-50 %	**0.1771**	0.2586	0.3393	0.2359	**1.0034**	0.8173	0.6931	0.8148	5697.1	**1911.2**	2513.3	2838.3
160–30-50 %	**0.2334**	0.3577	0.4516	0.3350	**1.0454**	0.7870	0.6711	0.7956	5230.6	**1848.8**	2289.4	2556.1
160–40-50 %	**0.1875**	0.2468	0.3171	0.2481	**1.0559**	0.8795	0.7433	0.8437	5710.7	**2044.1**	2625.5	2893.0

Table 7
Average results of IGD, HV, and Time of four algorithms on instances where the percentage of customers served by drones is 70%.

Instance	IGD				HV				Time(s)			
	E	N	S	M	E	N	S	M	E	N	S	M
40–20-70 %	**0.1801**	0.2739	0.2519	0.2896	**0.8832**	0.7633	0.8740	0.7980	1238.2	510.2	**504.6**	536.9
40–30-70 %	**0.1588**	0.2178	0.1932	0.1960	**0.8807**	0.6948	0.8119	0.8048	1224.2	**507.7**	526.6	532.1
40–40-70 %	**0.2283**	0.3197	0.3023	0.2749	**0.8728**	0.7061	0.7732	0.7615	1196.6	572.2	592.6	**543.2**
80–20-70 %	**0.1936**	0.2608	0.2679	0.2971	**0.9621**	0.7936	0.7940	0.7199	3268.9	**1099.4**	1272.4	1530.2
80–30-70 %	**0.2354**	0.3919	0.3666	0.3859	**1.0170**	0.7324	0.8103	0.7751	3323.5	**1144.7**	1266.9	1578.5
80–40-70 %	**0.3232**	0.4228	0.5032	0.4923	**1.0262**	0.8280	0.7718	0.6918	2999.8	**1157.4**	1267.3	1533.2
120–20-70 %	**0.2857**	0.3637	0.3819	0.3461	**0.8953**	0.7415	0.7108	0.7650	5251.5	**1697.3**	2100.2	2584.8
120–30-70 %	**0.2304**	0.4297	0.5110	0.3720	**1.0063**	0.7347	0.6586	0.7460	5372.9	**1829.1**	2125.3	2697.7
120–40-70 %	**0.2543**	0.4017	0.3905	0.4296	**1.0324**	0.7266	0.7408	0.6393	5006.9	**1773.5**	2223.1	2622.1
160–20-70 %	**0.2135**	0.2849	0.3580	0.2364	**0.9695**	0.7729	0.6822	0.8284	7567.3	**2454.6**	3072.4	3775.9
160–30-70 %	**0.2011**	0.2863	0.3546	0.3100	**1.0017**	0.8323	0.7295	0.7652	7837.1	**2508.6**	3213.4	3919.9
160–40-70 %	**0.1782**	0.2935	0.3987	0.3038	**1.0869**	0.8156	0.6807	0.7634	7368.8	**2604.2**	3158.1	3834.0

Table 8
Average results of C-metric of ENSGA-II vs other algorithms on instances where the percentage of customers served by drones is 70%.

Instance	ENSGA-II (E) vs NSGA-II (N)		ENSGA-II (E) vs SPEA2 (S)		ENSGA-II (E) vs MOEA\D (M)	
	C (E, N)	C (N, E)	C (E, S)	C (S, E)	C (E, M)	C (M, E)
40–20-70 %	**0.4678**	0.1669	**0.4239**	0.0862	**0.4288**	0.0950
40–30-70 %	**0.4189**	0.1400	**0.4509**	0.1200	**0.3699**	0.1019
40–40-70 %	**0.4964**	0.1217	**0.5088**	0.1974	**0.5725**	0.0962
80–20-70 %	**0.4594**	0.1263	**0.5681**	0.1175	**0.5826**	0.0413
80–30-70 %	**0.4588**	0.0620	**0.5890**	0.1369	**0.5268**	0.0863
80–40-70 %	**0.5127**	0.1329	**0.6308**	0.1262	**0.7251**	0.0875
120–20-70 %	**0.3841**	0.1544	**0.5955**	0.1225	**0.4067**	0.1312
120–30-70 %	**0.5658**	0.1115	**0.6529**	0.1326	**0.5045**	0.1315
120–40-70 %	**0.6997**	0.0877	**0.6840**	0.0791	**0.7940**	0.0383
160–20-70 %	**0.5017**	0.2307	**0.6525**	0.1029	**0.4179**	0.1597
160–30-70 %	**0.4304**	0.2007	**0.6301**	0.0963	**0.4733**	0.1712
160–40-70 %	**0.6631**	0.1396	**0.7781**	0.0701	**0.7294**	0.1250

Table 9
Statistical results of Wilcoxon rank sum test for performance difference between ENSGA-II vs other algorithms.

Performance indicator	ENSGA-II vs NSGA-II	ENSGA-II vs SPEA2	ENSGA-II vs MOEA\D
HV	36/0	31/5	35/1
IGD	34/2	31/5	33/3
C-metric	30/6	36/0	31/5

solutions. C (S_1, S_2) is defined as the ratio of the solutions in S_2 that are dominated by at least one solution in S_1. For example, C (S_1, S_2) = 1 means that all solutions in S_2 are dominated by at least one solution in S_1. In particular, C (S_2, S_1) is not equal to 1 – (S_1, S_2).

5.3. Experimental results

To comprehensively evaluate the performance of ENSGA-II compared with the three other baseline algorithms, experiments were conducted on 36 instances. Each algorithm ran independently for 20 times on the same instance to reduce the effect of randomness on experimental results. The average values were taken as the results of the performance indicators.

Some details of the experiments are set as follows: (1) Because the true Pareto front of instances is unknown, all non-dominated solutions obtained by the four algorithms are regarded as the true Pareto front of instances by calculating IGD. (2) The reference point R was set to [1.1, 1.1, 1.1] in calculating HV. (3) The objectives must be normalized owing to their different value ranges. (4) According to the trial experiments, the parameters of each algorithm were set in Table 2.

Table 10
Average rank of four algorithms using Friedman test on all instances in terms of HV and IGD.

HV	Average rank	Final rank	IGD	Average rank	Final rank
ENSGA-II	1.03	1	ENSGA-II	1.00	1
NSGA-II	3.00	3	NSGA-II	3.08	3
SPEA2	3.39	4	SPEA2	3.31	4
MOEA\D	2.58	2	MOEA\D	2.61	2

The experimental results are shown in Tables 3–8, with significant values of performance indicators marked in bold. ENSGA-II, NSGA-II, SPEA2, and MOEA\D algorithms are represented as "E," "N," "S," and "M," respectively in the columns of the tables. Tables 3, 5, and 7 present the average results of IGD, HV, and CPU computing time, respectively (represented by "Time", in seconds). Tables 4, 6, and 8 present the average results of the C-metric between ENSGA-II and the other three baseline algorithms.

Tables 3, 5, and 7 show that the IGD and HV of the ENSGA-II algorithm are better than those of the other algorithms in all instances. Tables 4, 6 and 8 also show that the quality of the non-dominated solutions obtained by the ENSGA-II algorithm is better than that obtained by the other algorithms for all instances. Therefore, based on the average results of the four algorithms, it can be concluded that the ENSGA-II algorithm can obtain high-quality solutions and has better diversity and convergence than the other three baseline algorithms. Because a multi-dimensional local search strategy is employed in the ENSGA-II algorithm, its CPU computing time is inevitably more than that of the other three algorithms. However, the additional computing time of ENSGA-II algorithm is still within an acceptable time range, and this weakness will be alleviated with advances in computer hardware and parallel computation techniques.

5.4. Experimental analysis

Although ENSGA-II algorithm achieves the best performance values (HV and IGD) among four algorithms, it is still not rigorous to infer the superiority of the ENSGA-II algorithm only from the average results. Therefore, Wilcoxon rank sum test (Wilcoxon, 1992) and Friedman test (Friedman, 1940) are conducted at 5 % significance level to verify the significant advantage of ENSGA-II algorithm over other three algorithms in solving given instances.

The statistical results of the Wilcoxon rank sum test are shown in Table 9. The result values *num1/num2* indicate that ENSGA-II has a

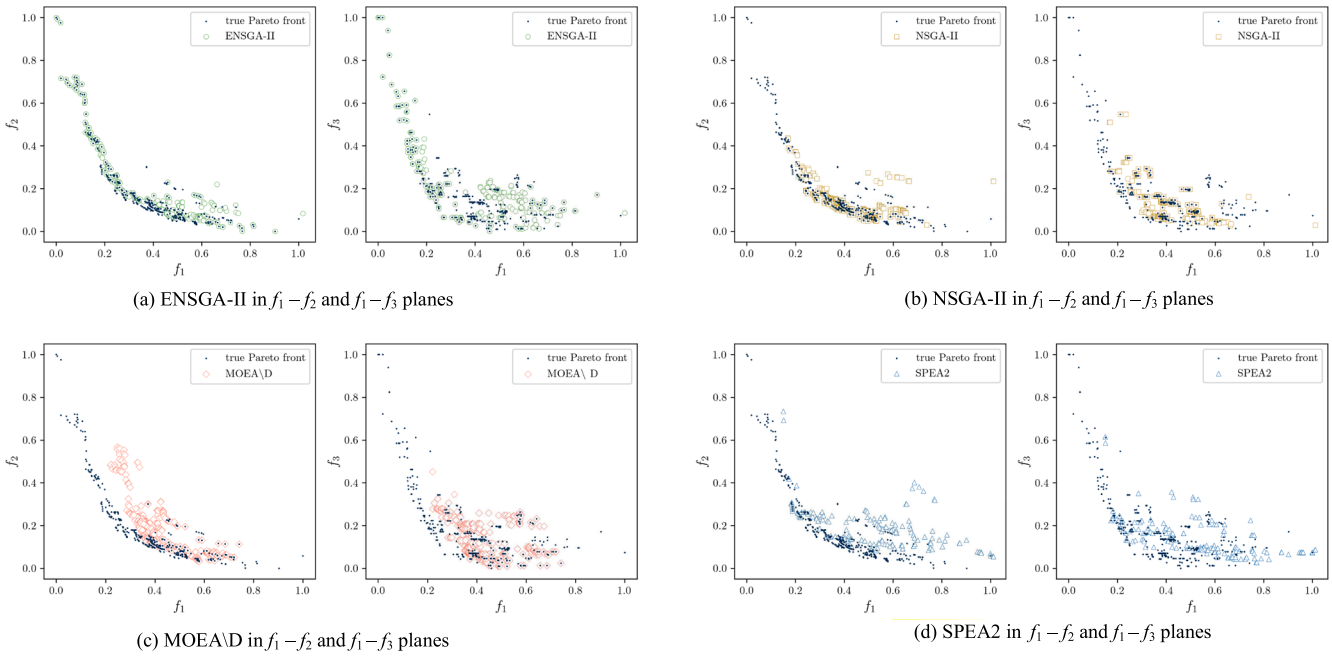

(a) ENSGA-II in f_1-f_2 and f_1-f_3 planes

(b) NSGA-II in f_1-f_2 and f_1-f_3 planes

(c) MOEA\D in f_1-f_2 and f_1-f_3 planes

(d) SPEA2 in f_1-f_2 and f_1-f_3 planes

Fig. 8. Plots of approximate Pareto fronts obtained by four algorithms in 160–20-30% instances.

significant performance advantage over its comparison algorithm in *num1* instances, but not in *num2* instances. In general, ENSGA-II outperforms NGSA-II, SPEA2 and MOEA\D algorithms in most of the instances.

The statistical results of Friedman test are shown in Table 10. This test ranks the performance of the four algorithms in all instances in terms of HV and IGD. The results show that ENSGA-II ranks first, followed by MOEA\D, NGSA-II and SPEA2 algorithms.

To further describe the advantage of ENSGA-II algorithm, Fig. 8 visualizes the approximate Pareto fronts obtained by four algorithms in 160–20-30 % instances respectively. The f_1–f_2 plane and f_1–f_3 plane are two different views of the approximate Pareto front in the three-dimensional coordinate system $\{f_1, f_2, f_3\}$. The true Pareto front in Fig. 8 is assumed to consist of non-dominated solutions obtained by running all algorithms 20 times. It is obvious that the approximate Pareto front obtained by ENSGA-II is more widely distributed and closer to the true Pareto front. Therefore, ENSGA-II algorithm can obtain high-quality non-dominated solutions and has better diversity and convergence than the other three algorithms.

6. Conclusion

To enable the logistics providers in making trade-off decisions between economic benefits and environmental impact, this study proposes a novel multi-objective optimization model for the vehicle routing problem with drone delivery. In the proposed model, economic and environmental objectives are optimized simultaneously, by minimizing the total delivery costs, total delivery time, and total energy consumption of trucks. Furthermore, the dynamic flight endurance of drones which depends on the loading rate of drones is considered to satisfy practical application scenarios. To solve this complex model, the ENSGA-II algorithm which integrates new encoding and decoding methods, several crossover and mutation operators, and a multi-dimensional local search strategy, is presented to optimize the routes of both trucks and drones. In the experiments, the effectiveness of the ENSGA-II algorithm in solving the proposed model was verified by comparing it with three other baseline algorithms.

Although the proposed ENSGA-II algorithm is effective in obtaining higher quality non-dominated solutions, its efficiency needs to be further improved in future research. Future work will include the design of objective-specific mutation operators, which may further accelerate algorithmic convergence. In addition, uncertain factors such as customer demand or service time can be considered in the model to better adapt to the real world scenario.

7. Ethical standard

The authors state that this research complies with ethical standards. This research does not involve either human participants or animals.

CRediT authorship contribution statement

Shuai Zhang: Conceptualization, Methodology, Formal analysis, Writing – review & editing, Supervision, Funding acquisition. **Siliang Liu:** Methodology, Formal analysis, Writing – original draft, Software, Validation. **Weibo Xu:** Data curation, Software, Validation. **Wanru Wang:** Writing – review & editing, Supervision.

Declaration of Competing Interest

The authors declare that they have no known competing financial interests or personal relationships that could have appeared to influence the work reported in this paper.

Data availability

All experimental data for this research were uploaded to the Figshare database (https://doi.org/10.6084/m9.figshare.17697209).

Acknowledgements

This work was supported by the National Natural Science Foundation of China (No. 51975512), and Zhejiang Key R & D Project of China (No. 2021C03153).

References

Agatz, N., Bouman, P., & Schmidt, M. (2018). Optimization approaches for the traveling salesman problem with drone. *Transportation Science, 52*(4), 965–981.

Asghari, M., & Al-e-hashem, S. M. J. M. (2021). Green vehicle routing problem: A state-of-the-art review. *International Journal of Production Economics, 231*, Article 107899.
Chiang, W. C., Li, Y. Y., Shang, J., & Urban, T. L. (2019). Impact of drone delivery on sustainability and cost: Realizing the UAV potential through vehicle routing optimization. *Applied Energy, 242*, 1164–1175.
Chung, S. H., Sah, B., & Lee, J. (2020). Optimization for drone and drone-truck combined operations: A review of the state of the art and future directions. *Computers & Operations Research, 123*, Article 105004.
Das, D. N., Sewani, R., Wang, J., & Tiwari, M. K. (2021). Synchronized truck and drone routing in package delivery logistics. *IEEE Transactions on Intelligent Transportation Systems., 22*, 5772–5782.
Deb, K., Pratap, A., Agarwal, S., & Meyarivan, T. (2002). A fast and elitist multiobjective genetic algorithm: NSGA-II. *IEEE Transactions on Evolutionary Computation, 6*, 182–197.
Dorling, K., Heinrichs, J., Messier, G. G., & Magierowski, S. (2017). Vehicle routing problems for drone delivery. *IEEE Transactions on Systems, Man and Cybernetics-Systems, 47*(1), 70–85.
Erdoğan, S., & Miller-Hooks, E. (2012). A green vehicle routing problem. *Transportation Research Part E-Logistics and Transportation Review, 48*(1), 100–114.
Fan, H. M., Zhang, Y. G., Tian, P. J., Lv, Y. C., & Fan, H. (2021). Time-dependent multi-depot green vehicle routing problem with time windows considering temporal-spatial distance. *Computers & Operations Research, 129*, Article 105211.
Friedman, M. (1940). A comparison of alternative tests of significance for the problem of m rankings. *The Annals of Mathematical Statistics, 11*(1), 86–92.
Goldberg, D. (1989). *Genetic Algorithms in Search, Optimization and Machine Learning*. Boston, Massachusetts: Addison Wesley.
Ha, Q. M., Deville, Y., Pham, Q. D., & Hà, M. H. (2018). On the min-cost traveling salesman problem with drone. *Transportation Research Part C-Emerging Technologies, 86*, 597–621.
Jabir, E., Panicker, V. V., & Sridharan, R. (2015). Multi-objective optimization model for a green vehicle routing problem. *Procedia-Social and Behavioral Sciences, 189*, 33–39.
Kara, İ., Kara, B. Y., & Yetis, M. K. (2007). Energy minimizing vehicle routing problem. *In Proceedings of the 1st International Conference on Combinatorial Optimization and Applications*, August 14-16, Xi'an, China, 62-71.
Karak, A., & Abdelghany, K. (2019). The hybrid vehicle-drone routing problem for pick-up and delivery services. *Transportation Research Part C-Emerging Technologies, 102*, 427–449.
Kitjacharoenchai, P., Ventresca, M., Moshref-Javadi, M., Lee, S., Tanchoco, J. M., & Brunese, P. A. (2019). Multiple traveling salesman problem with drones: Mathematical model and heuristic approach. *Computers & Industrial Engineering, 129*, 14–30.
Li, H. Q., Wang, H. T., Chen, J., & Bai, M. (2020). Two-echelon vehicle routing problem with time windows and mobile satellites. *Transportation Research Part B-Methodological, 138*, 179–201.
Li, J., Wang, D. P., & Zhang, J. H. (2018). Heterogeneous fixed fleet vehicle routing problem based on fuel and carbon emissions. *Journal of Cleaner Production, 201*, 896–908.
Li, Y. B., Soleimani, H., & Zohal, M. (2019). An improved ant colony optimization algorithm for the multi-depot green vehicle routing problem with multiple objectives. *Journal of Cleaner Production, 227*, 1161–1172.
Moshref-Javadi, M., Hemmati, A., & Winkenbach, M. (2021). A comparative analysis of synchronized truck-and-drone delivery models. *Computers & Industrial Engineering, 162*, Article 107648.
Murray, C. C., & Chu, A. G. (2015). The flying sidekick traveling salesman problem: Optimization of drone-assisted parcel delivery. *Transportation Research Part C-Emerging Technologies, 54*, 86–109.
Murray, C. C., & Raj, R. (2020). The multiple flying sidekicks traveling salesman problem: Parcel delivery with multiple drones. *Transportation Research Part C-Emerging Technologies, 110*, 368–398.
Potvin, J. Y. (1996). Genetic algorithms for the traveling salesman problem. *Annals of Operations Research, 63*(3), 337–370.
Prins, C. (2004). A simple and effective evolutionary algorithm for the vehicle routing problem. *Computers & Operations Research, 31*, 1985–2002.
Prins, C., Labadi, N., & Reghioui, M. (2009). Tour splitting algorithms for vehicle routing problems. *International Journal of Production Research, 47*(2), 507–535.
Sacramento, D., Pisinger, D., & Ropke, S. (2019). An adaptive large neighborhood search metaheuristic for the vehicle routing problem with drones. *Transportation Research Part C-Emerging Technologies, 102*, 289–315.
Schneider, M., Stenger, A., & Goeke, D. (2014). The electric vehicle-routing problem with time windows and recharging stations. *Transportation Science, 48*(4), 500–520.
Tian, X., Geng, Y., Zhong, S. Z., Wilson, J., Gao, C. X., Chen, W., … Hao, H. (2018). A bibliometric analysis on trends and characters of carbon emissions from transport sector. *Transportation Research Part D-Transport and Environment, 59*, 1–10.
Trop, J. (2016). Drone delivery is about to disrupt the trucking industry. https://www.trucks.com/2016/06/21/drone-delivery-reshape-trucking/.
Turkensteen, M. (2017). The accuracy of carbon emission and fuel consumption computations in green vehicle routing. *European Journal of Operational Research, 262*(2), 647–659.
Wang, J., Yao, S., Sheng, J. C., & Yang, H. T. (2019). Minimizing total carbon emissions in an integrated machine scheduling and vehicle routing problem. *Journal of Cleaner Production, 229*, 1004–1017.
Wang, X. Y., Poikonen, S., & Golden, B. (2017). The vehicle routing problem with drones: Several worst-case results. *Optimization Letters, 11*(4), 679–697.
Wei, F. Q., Zhang, X. Q., Chu, J. F., Yang, F., & Yuan, Z. (2021). Energy and environmental efficiency of China's transportation sectors considering CO2 emission uncertainty. *Transportation Research Part D-Transport and Environment, 97*, Article 102955.
Wilcoxon, F. (1992). Individual comparisons by ranking methods. In U. S. A. New York (Ed.), *Breakthroughs in Statistics* (pp. 196–202). Springer.
Xiao, Y. Y., Zhao, Q. H., Kaku, I., & Xu, Y. C. (2012). Development of a fuel consumption optimization model for the capacitated vehicle routing problem. *Computers & Operations Research, 39*(7), 1419–1431.
Xu, Z. T., Elomri, A., Pokharel, S., & Mutlu, F. (2019). A model for capacitated green vehicle routing problem with the time-varying vehicle speed and soft time windows. *Computers & Industrial Engineering, 137*, Article 106011.
Zhang, Q. F., & Li, H. (2007). MOEA/D: A multiobjective evolutionary algorithm based on decomposition. *IEEE Transactions on Evolutionary Computation, 11*, 712–731.
Zhang, S., Chen, M. Z., Zhang, W. Y., & Zhuang, X. Y. (2020). Fuzzy optimization model for electric vehicle routing problem with time windows and recharging stations. *Expert Systems with Applications, 145*, 113123.
Zhang, Z., Qin, H., & Li, Y. (2019). Multi-objective optimization for the vehicle routing problem with outsourcing and profit balancing. *IEEE Transactions on Intelligent Transportation Systems, 21*(5), 1987–2001.
Zitzler, E., & Thiele, L. (1999). Multiobjective evolutionary algorithms: A comparative case study and the strength Pareto approach. *IEEE Transactions on Evolutionary Computation, 3*(4), 257–271.
Zitzler, E., Laumanns, M., & Thiele, L. (2002). SPEA2: Improving the strength pareto evolutionary algorithm. *Evolutionary Methods for Design, Optimization and Control*, Barcelona, Spain: CIMNE, 95-100.